

A Study on Mathematical Model of Turbulent Combusting Flow Using Amr (Adaptive Mesh Refinement) Algorithms

J. Mugaibullah

Assistant Professor, Department of Mathematics

Pollachi College Of Arts And Science, Poosaripatti (Pollachi)

ABSTRACT

The Study on mathematical model of turbulent combusting flows by usig AMR Algorithms. Due to more manageable computational requirements and somewhat greater ease in handling complex flow geometries, most practical simulation algorithms are based on the Reynolds- or Favre-averaged Navier–Stokes equations, where the turbulent flow structure is entirely modelled and not resolved. The time-averaging approach, the system of equations governing turbulent combusting flows can be both large and stiff and its solution can still place severe demands on available computational resources.

KEYWORDS: Turbulent Combusting Flows, Navier–Stokes equations, AMR Algorithms

1. INTRODUCTION

Introduction of mathematical model of turbulent combusting flows by usig AMR Algorithms have been taken to reduce the computational costs of simulating combusting flows. One successful approach is to make use of solution-directed mesh adaptation, such as the adaptive mesh refinement (AMR) algorithms developed for aerospace applications Berger and Saltzman 1994, Aftosmis et al. 1998, Groth et al. 1999, 2000, Sachdev et al. 2005). Computational problems with disparate length scales, providing the required spatial resolution while minimising memory and storage requirements. Recent progress in the development and application of AMR algorithms. The producing a parallel AMR method that both reduces the overall problem size and the time to calculate a solution for laminar combusting flows. The extension of this combined approach to turbulent non-premixed combusting flows is the focus of this study.

2. PRELIMINARIES

2.1 Fluid Dynamics

Fluid dynamics is a subdisciplines of fluid mechanics that describes the **flow of fluids**-liquid and gases. It has several subdisciplines, including **aerodynamics** (the study of air and other gases in motion) and **hydrodynamics** (the study of liquid in motion). The father of fluid dynamics is **blaise pascal**.

2.2 Turbulent Flow

A type of fluid (gases or liquid) flow in which the fluid undergoes irregular fluctuations, or mixing, in contrast to laminar flow, in which fluid moves **in smooth paths of layers**. In **turbulent flow** the speed of the fluid at a point is continuously undergoing changes in both **magnitude and directions**.

2.3 Navier-Stokes Equations

In fluid dynamics a partial differential equations that describes the flow of incompressible fluids. The equation is a generalization of the equation devised **swiss mathematicians Leonhard euler** in the 18thcentuary to describes the flow of incompressibleand frictionless fluid

$$\frac{\partial u}{\partial t} + \frac{(u \cdot \nabla) u}{\rho} = - \frac{1}{\rho} \nabla p + \nu \nabla^2 u$$

2.4 Inviscid Fluid

Inviscid flow is the flow of an inviscid fluid, in which the viscosity of the fluid isequal to zero. When viscous force are neglected such as the case of the inviscid flow.

2.5 Viscous Flow

A type of fluid flow in which there is a **continuous steady motion** of the particle; the motion at a fixed point is **always remains constant**. Also called **streamlines flow; laminar flow; steady flow**.

2.6 Turbulent Prandtl Number

A dimensionless parameter used in calculations of heat transfer between a moving fluid and a solid body equal to $C_p V/K$, Where C_p is the heat capacity per unit volume, V is the kinematic viscosity, K is thermal conductivity.

2.7 Reynolds Number

Reynold number is the ratio of **inertial forces to viscous force** within a fluid which is subjected to relative **internal moment due to different fluid velocities**, which is known as a boundary layer in the case of a boundary surface such as the interior of a pipe.

2.8 Eddy Viscosity

The turbulent transfer of momentum by eddies giving rise to an internal fluid friction, in a manner analogous to the **action of molecular viscosity in laminar flow**, but taking place on a much larger scale. Eddy viscosity is a function of the **flow**, not of the **fluid**.

2.9 Molecular stress tensor or Viscous stress tensor

The viscous stress tensor is a tensor used in **continuum mechanics** to model the part of the stress at a point within some **material that can be attributed to the strain rate**, the rate at which it is deforming around that point.

2.10 Vorticity Tensor

Vorticity is generated at **solid interface** and at **fluid – fluid interfaces**. The vorticity tensor is a skew symmetric tensor. We can write its components in terms of the components of the velocity gradient in a rectangular cartesian basis set as follow.

3. MATHEMATICAL MODEL OF TURBULENT COMBUSTING FLOW

3.1 FAVRE-AVERAGED NAVIER–STOKES EQUATIONS

A mathematical model based on the Favre-averaged Navier–Stokes equations for a compressible thermally perfect reactive mixture of gases has been formulated and is used here in to describe turbulent non-premixed combustion processes. In this formulation, the continuity, momentum and energy equations for the reactive mixture of N species are

$$-\frac{\partial \rho}{\partial t} + \nabla \cdot (\rho \bar{u}) = 0 \tag{1}$$

$$\frac{\partial}{\partial t} (\bar{\rho} e) + \nabla \cdot (\bar{\rho} \bar{u} e + \bar{p} \bar{l}) = \nabla \cdot (\bar{\tau} + \bar{\lambda}) + \bar{f}, \tag{2}$$

where ρ is the time-averaged mixture density, \bar{u} is the Favre-averaged mean velocity of the mixture, p is the time-averaged mixture pressure, $e = \frac{|\bar{u}|^2}{2} + \sum_{n=1}^N c_n h_n - p/\rho + k$ is the Favre-averaged total specific mixture energy, \bar{f} is a body force per unit volume acting on the gaseous mixture, k is the specific turbulent kinetic energy, D_k is the coefficient for the diffusion of the turbulent energy, $\bar{\tau}$ and $\bar{\lambda}$ are the molecular and turbulent Reynolds stress tensors or dyads, and \bar{q} and \bar{q}_t are the molecular and turbulent heat flux vectors, respectively. Fourier’s law is used to represent the thermal diffusion caused by the random thermal motion and turbulence. In addition, h_n is the absolute (chemical and sensible) internal enthalpy for species n. The transport equation describing the time evolution of the species mass fraction, c_n , is given by

$$\frac{\partial}{\partial t} (\rho c_n) + \nabla \cdot (\rho c_n \bar{u}) = -\nabla \cdot (\bar{J}_n + \bar{J}_t) + \rho \bar{w}_n \tag{3}$$

Where \bar{w}_n is the time-averaged or mean rate of the change of the species mass fraction produced by the chemical reactions and \bar{J}_n and \bar{J}_t are the molecular and turbulent diffusive fluxes for species n, respectively. The latter are specified using Fick’s law. The modified two-equation $k-\omega$ model of Wilcox (2002) is used here to model the unresolved turbulent flow quantities. In this approach, the Boussinesq approximation is used to relate the Reynolds stress tensor, $\bar{\lambda}$, to the mean flow strain-rate tensor using a turbulent eddy viscosity, μ_t , with

$\mu_t = \frac{\rho k}{\omega}$. Transport equations are solved for turbulent kinetic energy, k , and the specific

dissipation rate, ω , given by

$$\frac{\partial}{\partial t}(\rho k) + \nabla \cdot (\bar{\rho} k u) = \lambda : \nabla u + \nabla \cdot [(\mu + \mu_t \sigma^*) \nabla k] - \beta^* \rho k \omega, \quad (4)$$

$$\frac{\partial}{\partial t}(\rho \omega) + \nabla \cdot (\rho \omega u) = \alpha \frac{\omega}{k} \lambda : \nabla u + \nabla \cdot [(\mu + \mu_t \sigma) \nabla \omega] - \beta \rho \omega^2, \quad (5)$$

where μ is the molecular viscosity of the mixture and $\beta^*, \sigma^*, \alpha, \beta$ and σ are close coefficients of this two-equation model. The latter are given by

$$\alpha = \frac{13}{25}, \quad \beta = \beta_0 f_\beta, \quad \beta^* = \beta_0^* f_\beta, \quad \sigma = \sigma^* = \frac{1}{2}, \quad (6)$$

with

$$\beta_0 = \frac{9}{125}, \quad \beta_0^* = \frac{9}{100}, \quad (7)$$

$$f_\beta = \frac{1+70 \chi_\omega}{1+80 \chi_\omega}$$

$$f_\beta = \left\{ \frac{1+680 \chi_k^2}{1+400 \chi_k} \right\} \quad (8)$$

For two-dimensional axisymmetric flows, the preceding equations can be re-expressed using vector notation as

$$\frac{\partial U}{\partial t} + \frac{\partial}{\partial r} (F - F_v) + \frac{\partial}{\partial z} (G - G_v) = \frac{1}{r} (S_\phi + S_{\phi_v}) + S \quad (9)$$

where U is the vector of conserved variables given by

$$U = [\rho, \rho v_r, \rho v_z, \rho e, \rho k, \rho \omega, \rho c_1, \dots, \rho c_N]^T \quad (10)$$

and F and F_v are the inviscid and viscous radial flux vectors, G and G_v are the inviscid and viscous axial flux vectors, S_ϕ and S_{ϕ_v} are the inviscid and viscous source vectors associated with the axisymmetric geometry, and S is the source vector containing terms related to the finite rate chemistry body forces, and turbulence modeling, respectively. Here r and z are the radial and axial coordinates of the axisymmetric frame and v_r and v_z are the radial and axial velocity components.

3.2 TREATMENT OF NEAR-WALL TURBULENCE

Both low-Reynolds-number and wall-function formulations of the $k-\omega$ model are used for the treatment of near-wall turbulent flows, with a procedure for automatically switching from one to the other, depending on mesh resolution. In the case of the low-Reynolds-number formulation, it can be shown that

$$\lim \omega = \frac{6\nu}{\sqrt{\beta} y^{3/2}} \tag{12}$$

where y is the distance normal from the wall. Rather than attempting to solve the ω - equation directly, the preceding expression is used to specify ω for all values of $y^+ \leq 2.5$,

where $y^+ = u_\tau y/\nu$, $u_\tau^2 = T_w/\rho$, and T_w is the wall shear stress. Provided there are 3–5 computational cells inside $y^+ = 2.5$, this procedure reduces numerical stiffness, guarantees numerical accuracy, and permits the $k-\omega$ model to be solved directly in the near-wall region without resorting to wall functions. In the

case of the wall-function formulation, the expression

$$k = \frac{u_\tau^2}{\sqrt{\beta_0}} \tag{13}$$

$$\omega = \frac{u_\tau}{\sqrt{\beta_0^*} ky} \tag{14}$$

are used to fully specify k and ω for $y^+ \leq 30-250$, where k is the von Kármán constant. The formulae

$$k = \frac{u_\tau^2}{\sqrt{\beta_0^*}} \left| \frac{y^+}{y_{cutoff}^+} \right|^2 \tag{15}$$

$$\omega = \omega_0 \sqrt{1 + \left(\frac{\omega_{cutoff}}{\omega_0} \right)^2} \tag{16}$$

have been devised to prescribe k and ω for y^+ lying between 2.5 and a cutoff value, y_{cutoff}^+ ,

where ω_0 and ω_{wall} are the values in the near-wall sub layer and in the log layer, respectively.

The cutoff, y_{cutoff}^+ , ω_0 is taken to be in the range 30–50 for this study. When y^+ is close to

3.3 PARALLEL AMR ALGORITHM

3.3.1 FINITE VOLUME SCHEME

A finite volume scheme is employed to solve the Favre averaged Navier–Stokes equations of equation (9) above for a two-dimensional axisymmetric coordinate frame. The system of governing equations is integrated over quadrilateral cells of a structured multi- block quadrilateral mesh. The semi-discrete form of this finite-volume formulation applied to cell (i, j) is given by

$$\frac{dU_{i,j}}{dt} = -\frac{1}{A_{i,j}} \sum_{faces,k} \vec{F}_{i,j,k} \cdot \vec{n}_{i,j,k} \Delta l_{i,j,k} + \frac{1}{r_{i,j}} (S_{\phi} + S_{\phi'}) + S_{I,j} \quad (17)$$

Where $F = (F - F_V, G - G_V)$, $r_{i,j}$ and $A_{i,j}$ are the radius and area of cell (i, j), and Δl and n are the length of the cell face and unit vector normal to the cell face or edge, respectively. The inviscid (hyperbolic) components of the numerical flux at each cell face is evaluated using limited linear reconstruction (Barth 1993) and one of several Riemann-solver used flux functions (Roe 1981, Einfeldt 1988, Linde 2002). The viscous (elliptic) components of the cell face flux are evaluated by employing a centrally weighted diamond-path reconstruction procedure as described by Coirier and Powell (1996).

For the time-invariant calculations performed as part of this study, a multi grid algorithm with multi-stage time marching scheme smoother is used to solve the coupled set of non-linear ordinary differential equations that arise from the finite-volume spatial discretization procedure. The smoother is based on the optimally-smoothing multistage time marching schemes developed by van Leer et al. (1989). To cope with numerical stiffness, a semi-implicit treatment is used in the temporal discretization of the source terms associated with axisymmetric geometry, finite-rate chemistry, turbulence modeling and gravitational acceleration.

3.3.2 BLOCK-BASED ADAPTIVE MESH REFINEMENT

AMR algorithms, which automatically adapt the mesh to the solution of the governing equations, can be very effective in treating problems with disparate length scales. They permit local mesh refinement and there by minimize the number of computational cells required for a particular calculation. Following the approach developed by Groth et al. (1999, 2000) for computational magneto hydrodynamics, a flexible block-based hierarchical data structure has been developed and is used in conjunction with the finite-volume scheme described above to facilitate automatic solution-directed mesh adaptation on multi block body-fitted quadrilateral mesh according to physics based refinement criteria. The method allows for anisotropic mesh refinement and is well suited to parallel implementation via domain decomposition. Refer to the recent papers by Sachdev et al. (2005) and Northrup and Groth (2005) for further details.

3.3.3 DOMAIN DECOMPOSITION AND PARALLEL IMPLEMENTATION

A parallel implementation of the block-based AMR scheme has been developed using the C++ programming language and the message passing interface (MPI) library

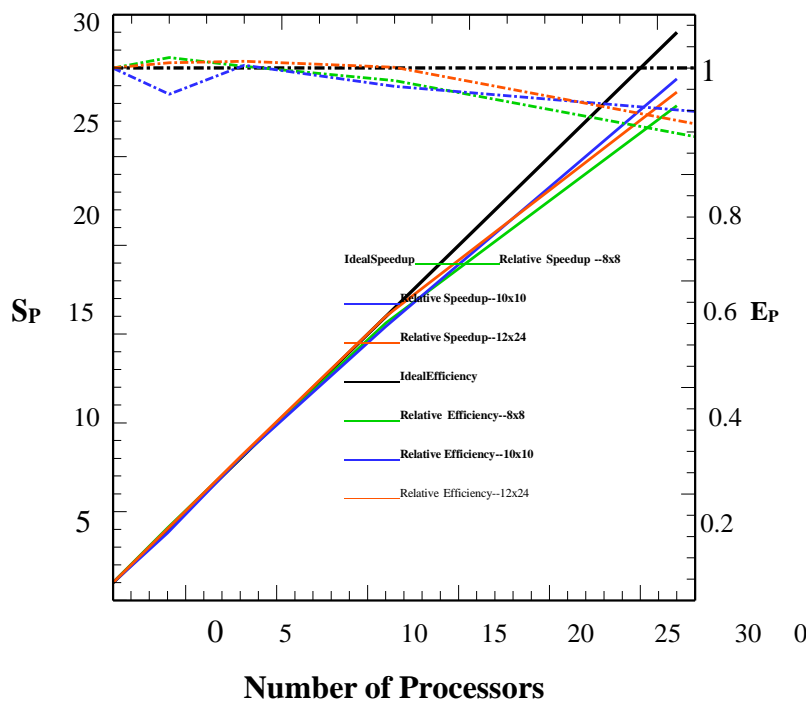


Figure 1. Relative parallel speed-up, S_p , and efficiency, E_p , for a fixed size problem using up to 32

by Gropp et al. (1999). A domain decomposition procedure is used where the solution blocks making up the computational mesh are distributed equally among available processors, with more than one block permitted per processor. A motion ordering space filling curve is used to order the blocks for more efficient load balancing (Aftosmis et al. 2004). The parallel implementation has been carried out on a parallel cluster of 4-way Hewlett-Packard ES40, ES45, and integrity rx4640 servers with a total of 244 Alpha and Itanium 2 processors. A low-latency performance and scalability of the proposed solution- adaptive method on this facility are shown in figure 1 for a fixed size turbulent non-reacting multi-species flow problem having 64 solution blocks. The relative parallel speed-up, S_p defined as

$$S_p = \frac{t_1}{t_p} P, \tag{18}$$

and the relative parallel efficiency, E_p , defined as

$$E_p = \frac{S_p}{P}, \tag{19}$$

are both shown in the figure, where t_1 is the processor time required to solve the problem using a single processor, and t_p is the total processor time required to solve the problem using p processors. The performance indicators are shown for three different mesh sizes: 4096 cells (64 8 x 8 cell blocks); 6400 cells (64 10 x 10 cellblocks); and 18,432 cells (64 12 x 24 cell blocks). It can be seen that the parallel speed-up of block-based AMR scheme is nearly linear and is about 87% for up to 32 processors, even for the smaller 8 x 8 cell solution blocks. The parallel efficiency is 92% for the larger 10 x 10 cell solution blocks.

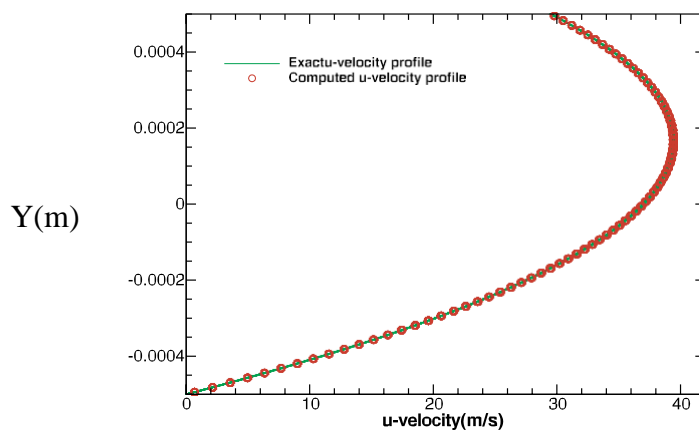


Figure 2. Comparison of predicted and exact solutions of the axial velocity profile for laminar Couette flow.

CONCLUSION

In this project the AMR scheme has been described for turbulent non-premixed combusting flows and parallel implementations also discussed the Navier stoke's equation of non-reacting and reacting flow results for the turbulent non-premixed flame bluff bodyburner.

REFERENCES

1. Aftosmis, M.J., Berger, M.J. and Melton, J.E., Robust and efficient Cartesian mesh generation for component-base geometry. AIAA J.,1998, 36, 952–960.
2. Aftosmis, M.J., Berger, M.J. and Murman, S.M., Applications of space filling curves to Cartesian methods for CFD. AIAA Pap., 2004, 2004–1232.
3. Barth, T.J., Recent developments in high order k-exact reconstruction on unstructured meshes. AIAA Pap., 1993, 93–668.
4. Bell, J.B., AMR for low Mach number reacting flow, 2004, <http://repositories.cdlib.org/lbnl/LBNL-54351>.
5. Bell, J.B., Day, M.S., Almgren, A.S., Lijewski, M.J. and Rendleman,C.A., Adaptive numerical simulation of turbulent premixed combustion. In Proceedings of the First MIT Conference on Computational Fluid and Solid Mechanics, June 2001.
6. Bell, J.B., Day, M.S., Almgren, A.S., Lijewski, M.J. and Rendleman,C.A., A parallel adaptive projection method for low Mach number flows. Int. J. Numer. Meth. Fluids, 2002, 40, 209–216.
7. Berger, M.J., Adaptive mesh refinement for hyperbolic partial differential equations. J. Comput. Phys., 1984, 53, 484–512.356 X. Gao and C. P. T. Groth
8. Berger, M.J. and Colella, P., Local adaptive mesh refinement for shock hydrodynamics. J. Comput. Phys., 1989, 82, 67–84.
9. Berger, M.J. and Saltzman, J.S., AMR on the CM-2. Appl. Numer. Math.,1994, 14, 239–253.
10. Coirier, W.J. and Powell, K.G., An adaptively-refined, Cartesian, cell based scheme for the Euler and Navier–Stokes equations. AIAA J.,1996, 34(5), 938–945.